Mechanism analysis of landslide of a layered slope induced by drawdown of water level

ZHANG Junfeng, LI Zhengguo & QI Tao

Institute of Mechanics, Chinese Academy of Sciences, Beijing 100080, China
Correspondence should be addressed to Zhang Junfeng (email: zhangjf@imech.ac.cn)
Received September 29, 2004

Abstract The frequent drawdown of water level of Yangtze River will greatly influence the stability of the widely existing slopes in the Three Gorges reservoir zone, especially those layered ones. Apart from the fluctuating speed of water level, the different geological materials will also play important roles in the failure of slopes. Thus, it must be first to study the mechanism of such a landslide caused by drawdown of water level.

A new experimental setup is designed to study the performance of a layered slope under the drawdown of water level. The pattern of landslide of a layered slope induced by drawdown of water level has been explored by means of simulating experiments. The influence of fluctuating speed of water level on the stability of the layered slope is probed, especially the whole process of deformation and development of landslide of the slope versus time. The experimental results show that the slope is stable during the water level rising, and the sliding body occurs in the upper layer of the slope under a certain drawdown speed of water level. In the process of slope failure, some new small sliding body will develop on the main sliding body, and the result is that they speed up the disassembly of the whole slope.

Based on the simulating experiment on landslide of a layered slope induced by drawdown of water level, the stress and displacement field of the slope are calculated. The seepage velocity, the pore water pressure, and the gradient of pore water head are also calculated for the whole process of drawdown of water level. The computing results are in good agreement with the experimental results. Accordingly, the mechanism of deformation and landslide of the layered slope induced by drawdown of water level is analyzed. It may provide basis for treating this kind of layered slopes in practical engineering.

Keywords: layered slope, landslide, drawdown of water level.

DOI: 10.1360/04zze24

1 Introduction

The instability of slopes on the river banks and the reactivation of ancient slopes, induced by drawdown of water level, are great danger for the local residents and for the

hydroelectric engineering. A lot of accidents or disasters relating to the drawdown of water level can be found in literatures. In October 1963, the landslide, near the recently constructed Vajont Reservoir dam at that time, caused the failure of the toppest hyperbolic arching dam in the world, ruined one city and several towns in the lower reach, and 1926 persons perished in the resulting flooding[1]. In July 1981, a flood that might occur nearly once every 100 years led to deformation of more than 100 loosely stacked geological layers from Chongqiong to Yichang, China. From 1965 to 1969, the deformation up to 10 m occurred in several sliding bodies in the upper reach of the Cepatsch dam (in Austria) during the early stage of the running of the reservoir. The Grand Coulee reservoir (in U.S.) also caused about 500 slopes to lose stability from 1942 to 1953. In China, the Three Gorges reservoir started conserving water from 2003. The water level of the reservoir would periodically fluctuate ranging from 135 to 175 m. The stability of the loosely stacked layers along the reservoir bank would be directly affected by the periodical drawdown of water level in addition to the other factors such as rainfall infiltration, the specific geomorphological and geological environment, the nonuniformity and stratification of rock soil, the faults and joints within the slopes, and the seepage and soakage in the geological materials[2−6].

Maoping sliding body, close to Geheyan Reservoir in Qingjiang, Hebei Province, China, began deforming after the water conservation in the reservoir in April 1993. Up to September 2001, the maximum displacement for the slope reached 2.1 m. About 3/4 of the first flat stair (about 180 m long, mainly composed of loose rock soil) was submerged in the water. According to the *in situ* monitoring results, the deformation responded quickly to the fall of water level but relatively slow to the rise of the water level. This means that the deformation is mainly affected by the fall of the water level. Though the deformation of Maoping sliding body is the synthetical result under both rainfall and drawdown of water level of Qingjiang river, the hydraulic effect and the reduction of strength of slope media are among the main factors to cause the occurrence of the landslide[7,8].

In Ref. [8], the authors considered the speed and the range of the fall of water level as the main factors to cause slopes sliding in the upper reach of the embankment. In order to explore the mechanism of landslide caused by drawdown of water level, the whole process of landslide (from deformation to sliding) for a layered slope was studied by experiment. The qualitative explanation for experimental phenomena had been given[9]. Numerical simulation was also conducted to reveal the change of some important parameters. The analysis in this paper is concentrated on the stress and displacement field of the slope, the seepage velocity, the pore water pressure, and the gradient of pore water head in order to probe the hydraulic effect during the change of water level. The resulting change of material strength for rock soil by water is not discussed here.

2 Experimental setup and layered slope

2.1 Experimental setup

In Ref. [10], a box, made of plexiglass material, with additional specific setup to supply

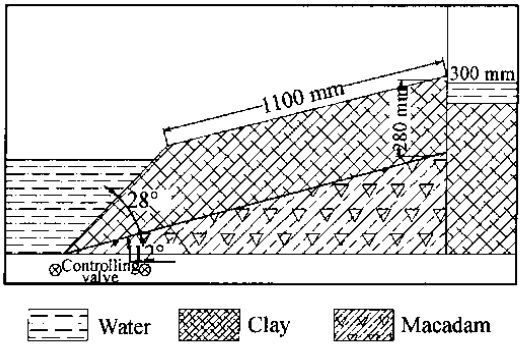

Fig. 1. Main experimental box for landslide study.

water in the upper reach of a slope model was used to study the slope failure by infiltration of rainwater. We also designed an experimental setup adopting high-transparent plexiglass material (Fig. 1). The thickness of the wall of the plexiglass box is 20 mm, and the inner size of the box is 2000 mm×800 mm×1100 mm (length× width× height). The bottom of the box was designed with a 100 mm sandwich layer and was covered with 5 mm steel plate in which equidistant holes (diameter 20 mm and space 50 mm) were arrayed. The steel plate was covered with a stainless steel net with 3 mm×3 mm mesh. The change of water level is controlled by injecting water into or drawing water out of the sandwich layer through a controlling valve. A smaller box (800 mm×300 mm×1100 mm) was also designed at one end in the main box to supply water in the upper reach of the slope model (see Fig. 1). Only on the side of the small box adjacent to the slope are there holes to permit supplying water to pass through.

2.2 Layered slope and parameters of the rock-soil material

By considering the geological configurations of the layered slopes, the experimental slope model was simplified but the main characteristics were retained: (a) The upper layer is of clay/silt to denote the weathered rock and soil (possibly mixed with crushed rock); (b) the second layer is of macadam to simulate the scree, gravel, or detritus, which indicates the unweathered stacked layer; (c) the fixed stainless steel net and plate in the bottom indicate the base rock. The initial size of the slope model is showed in Fig. 1. In order to have a good look at the deformation, some tracking point was set between the side of the slope model and the wall of the plexiglass box. The lattice designed with segment of thin cotton thread was also laid on the top surface of the slope model to measure the initiation of landslide and the sliding displacement conveniently.

The silt sample was adopted for the upper layer of the slope model because of its low cohesion (defined as c). Its main physical and mechanical properties were given here: the material density $\rho_s = 2.75\times10^3$ kg/m^3, the ratio of void $e = 1.8$, the natural dry density $\rho_d = 0.98\times10^3$ kg/m^3, the saturated density $\rho = 1.625\times10^3$ kg/m^3, the coefficient of permeability $K = 3.20\times10^{-6}$ m/s, the compressible coefficient 1.78 MPa^{-1}, the modulus of compression 1.935×10^6 N/m^2, index of liquidity 1.51, liquid limit 50.9, plastic limit 27.2, plastic index 23.7, coefficient of consolidation 7.2×10^{-4} cm/s; (a) quick shear test: $c = 10.4$ KPa, $\phi = 0.95°$; (b) consolidated quick shear test: $c_u = 14.5$ KPa, $\phi_u = 13°$. Triaxial test: (a) unconsolidated and undrained test: $c = 12$ KPa, $\phi = 0.57°$; (b) consolidated and drained test: $c_{cu} = 11.2$ KPa, $\phi_{cu} = 13.3°$. Unconfined compressive strength: (a) undisturbed $q_u = 20.45$ KPa; (b) recomposed $Q_u = 5.4$ KPa.

3 Experimental phenomena and results

By means of controlling the speed of injection and draining through the valve at the bottom of the main box, the change of water level with time in the lower reach is shown in Fig. 2. The slope was then stable after the process of several times consolidation and deformation at the initial slope angle 12°. The slope angle was slowly changed by lifting the right hand of the main box until it reached 23°. The water level was changed again and the whole process of deformation and sliding was recorded by using a digital camera.

When the water level changed with time (see Fig. 3), the following phenomena could be observed during the experimental process: The tensile cracks initiated on the top surface of the slope when the water level reached 300 mm in the lower reach of the slope (Fig. 4). Two minutes later, the length and width of the tensile cracks were up to 155 mm and 4 mm respectively, while the water level in the lower reach was 236 mm. Companied with the fall of the water level in the lower reach of the slope, the length and width of the tensile cracks increased quickly, a part of the slope body began to slide down and the sliding speed became quicker and quicker. A secondary sliding body separated from the main sliding body and it further speeded up the movement of the latter (Fig. 5). It was the secondary sliding body that caused the second peak value of speed in Fig. 6(b). As more and more sliding mass stacked at the foot of the slope, the sliding

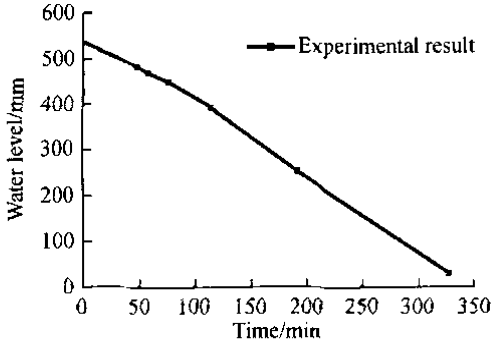

Fig. 2. Water level in the lower reach versus time.

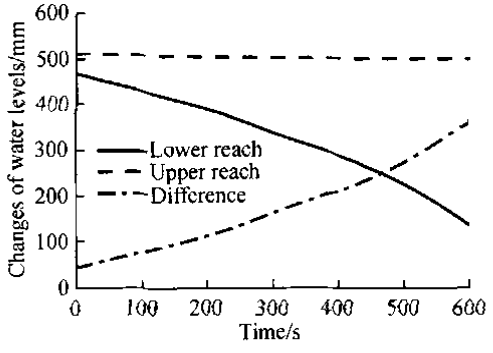

Fig. 3. Water level versus time.

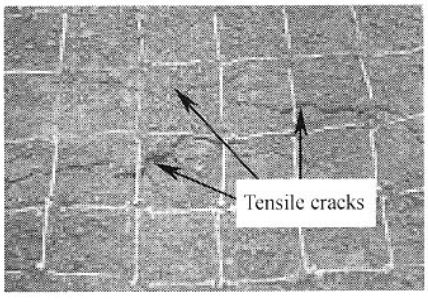

Fig. 4. Tensile cracks on the surface of slope.

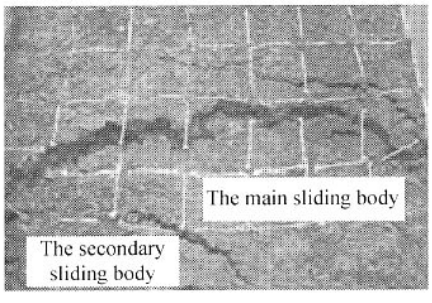

Fig. 5. The main and secondary sliding bodies.

body moved slower and slower and finally stopped. The whole process of deformation and landslide lasted about 20 min.

The sliding displacement and speed of landslide were obtained by analyzing the digital images. The results are shown in Fig. 6. The changes of the slope angle and the shape of the sliding surface could be observed from the side of the main experimental box. It could be seen that the shape of the sliding surface was nearly circular, and the slope angle of the sliding debris decreased by 5° compared with the initial slope angle.

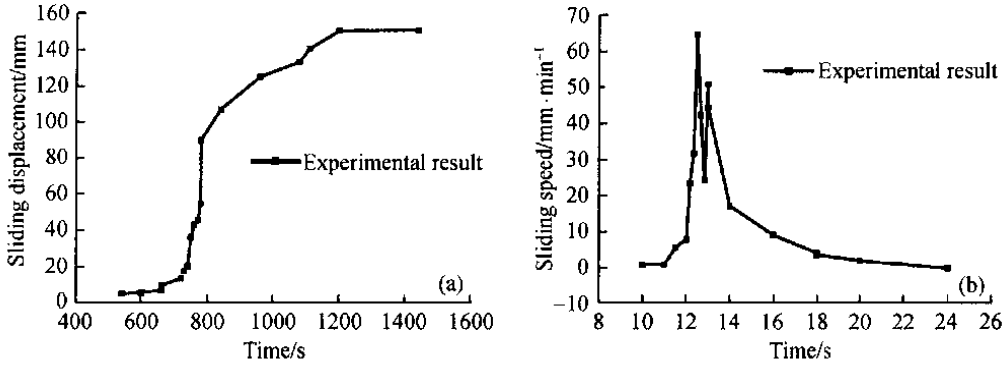

Fig. 6. (a) Sliding displacement versus time; (b) sliding velocity versus time.

4 Analysis of stress and displacement fields

The finite element method was adopted to analyze the static stress field and displacement field for the experimental slope model, and the size of the computing model was consistent with the experimental one (Fig. 1). Half of the full slope model was selected in analysis because the slope is geometrically symmetrical about the longitudinal central section, and this section was taken as symmetrical boundary. Contact element was used to simulate the interface between the upper and the lower layers. The wall of the main box was assumed as rigid shell and contact element was also used to simulate the interfaces between the wall of the box and the two soil layers. The 8-node solid element was adopted to divide the slope body, and the parameters of materials were identical to that in section 2.2 above. The computational model of mesh is shown in Fig. 7.

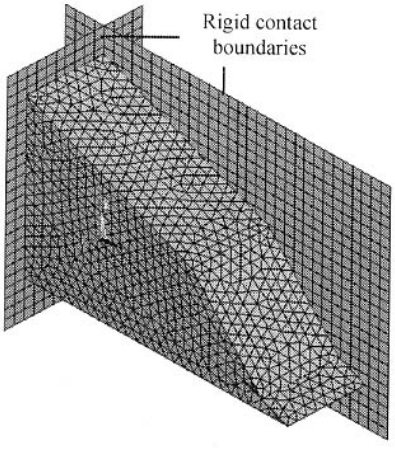

Fig. 7. Computational model of mesh.

The contours of Von Mises stress and the displacement field are shown in Fig. 8. It can be seen from Fig. 8(b) that the contours of displacement field are parallel to the tensile cracks on the top surface of the slope and the shape of one of the

contours of displacement is the same as that of the sliding body (Fig. 5). Some tensile cracks also developed behind the sliding body in the area of relatively large deformation.

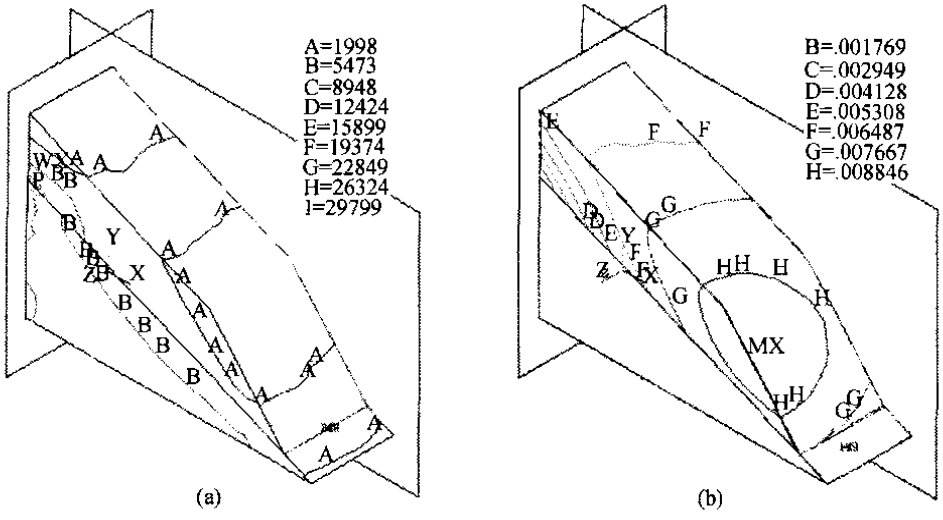

Fig. 8. (a) Contours of Von Mises stress (Pa); (b) contours of the displacement field (mm).

5 Change of the fields of seepage and pore water pressure

The drawdown of water level is one of the main factors to cause landslides. The hydraulic effect of the drawdown of water level is exhibited by means of the changes of seepage field and the pore water pressure field within the slope body. For the experimental slope model, the permeability of the upper layer is low. In addition to the water supply in the upper reach of the slope, the change of water table within the upper layer in a short time would be negligible. However, the rapid fall of the water level in the lower reach causes a sharp change for the gradient of the pore water pressure within the slope, especially in the vicinity of the foot of the slope. Therefore, the hydraulic effect is the main reason to cause the occurrence of landslide.

The finite element meshing for computing the fields of seepage and pore water pressure is shown in Fig. 9. The coefficients of permeability used in computation are k_s = 3.2×10^{-6} m/s for the upper layer and k_g = 1.0×10^{-2} m/s for the lower layer. The known water heads for the upper and the lower reaches are provided and the bottom boundary condition along with other boundaries is free. The change of the saturated water table (i.e. the water head being zero) with time is given in Fig. 10. It is shown that the change of the saturated water table is small even if the water level in the lower reach of the slope fell rapidly, because of, just as the description in the above paragraph, the unchanged water level in the upper reach and the low permeability of the upper layer. The distributions of the pore water pressure, the seepage velocity, and the gradient of pressure head are given for two cases. The first is for the moment when the water level in the

lower reach (h = 46.8 cm) began to fall (t = 0) (Fig. 11). The second is for the moment when the water level in the lower reach reached 13.8 cm at t = 600 s (Fig. 12). It should be noted that the computing water tables in Figs. 11 and 12 mean the contours of the computing water head being zero. The negative pore water head above the computing water table indicated the unsaturated state in this area.

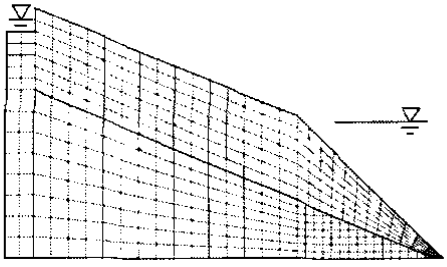

Fig. 9. Computational meshes for seepage.

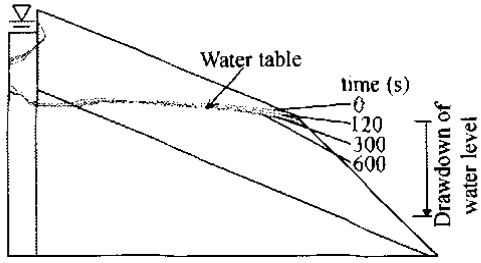

Fig. 10. Change of water table versus time.

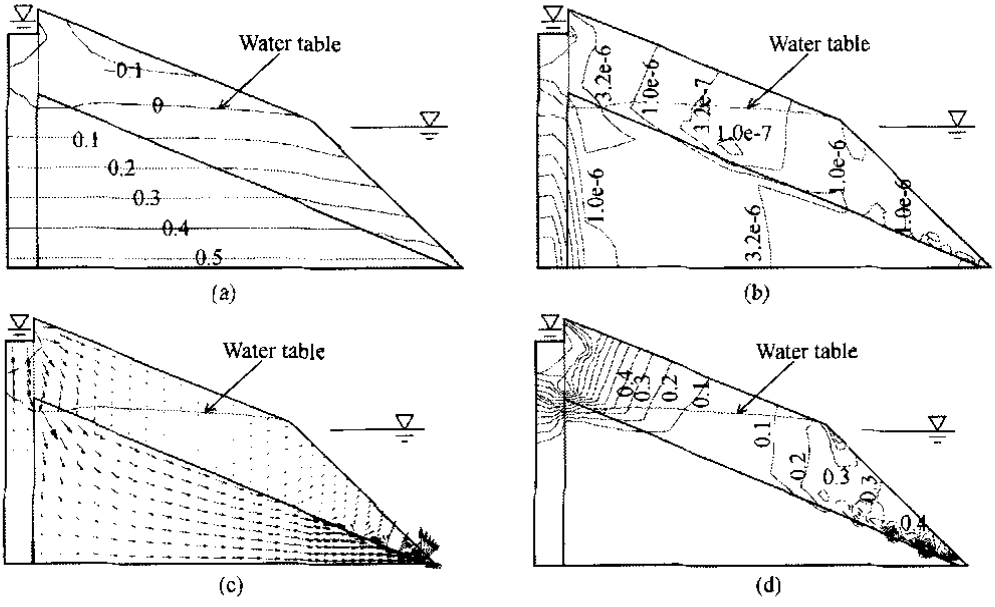

Fig. 11. Pressure head and seepage field (initial water level in the lower reach: 46.8 cm). (a) Contours of water head (m); (b) contours of seepage velocity (m/s); (c) seepage field of the slope; (d) contours of gradient of pressure head.

Comparing the computing results of the two cases with the water level difference being the largest, there are obvious differences in the distributions of the pore water pressure (Figs. 11(d) and 12(d)) and the seepage velocity (Figs. 11(b) and 12(b)) respectively. In this experiment, the tensile cracks initiated when the height of water level in the lower reach was 300 mm with t = 370 s. Hence, it is necessary to analyze the distributions of the pore water pressure and the seepage velocity at this moment (Fig. 13).

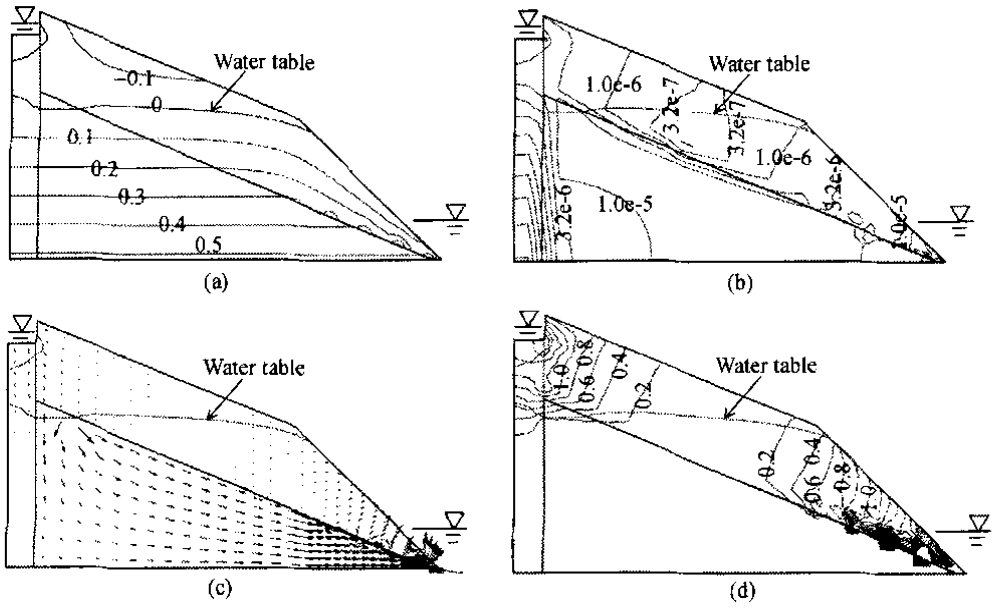

Fig. 12. Pressure head and seepage field (water level in the lower reach: 13.8 cm). (a) Contours of water head (m); (b) contours of seepage velocity (m/s); (c) seepage field of the slope; (d) contours of gradient of pressure head.

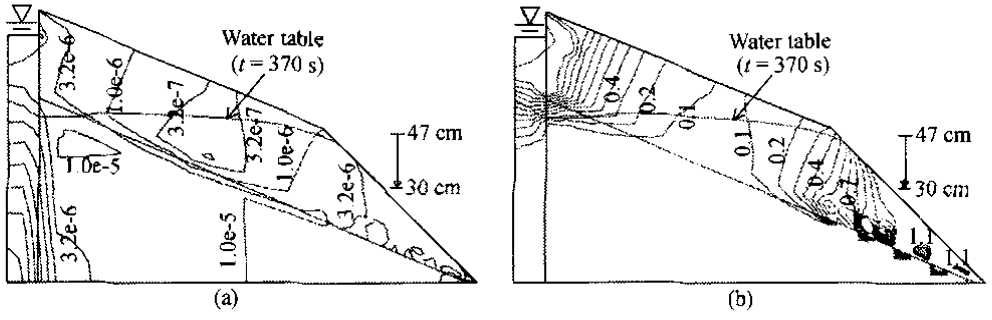

Fig. 13. Gradient of pressure head and seepage field (water level of low reach: 30 cm). (a) Contours of seepage velocity (m/s); (b) contours of gradient of pressure head.

6 Mechanism of landslide of a layered slope by drawdown of water level

Comparing the results in Figs. (11)—(13), the following conclusions can be drawn for the simulating experiment: (1) The gradient of pore water pressure and the seepage velocity in the vicinity of the foot of the slope were always larger than those in the other part of the slope before and after the fall of the water level, especially when the water level reached to a low level (Fig. 12(d)). The seepage pressure, a common saying for the gradient of pore water pressure in slope engineering, is one of the factors to cause landslide. (2) During the process of the fall of the water level, the gradient of pore water pressure near the steep surface and the foot of the slope increased quickly, which means the dynamic pore water pressure taking effect. That is another factor to cause landslide

(Figs. 11(d), 12(d), and 13(b)). (3) The contours of seepage velocity near the steep surface and the foot of the slope in Figs. 12(b) and 13(a) are obviously larger than those in Fig. 11(b). It indicates that the dynamic pore water pressure after the fall of the water level is larger than that before the fall of the water level.

In this experiment, the gradient of water pressure in the lower layer (macadam) would be small for the permeability is relatively large during the change of the water level. Contrarily, for the upper layer with low permeability, water was continuously supplied from the small box in the upper reach, and there was no time for the pore water to seep out during the rapid fall of the water level. Hence, the large gradient of pore water pressure developed in this layer as shown in Figs. 11(d), 12(d), and 13(b). The tensile deformation initiated on the top surface of the slope under the action of gravity and static/dynamic pore water pressure, then the tensile deformation developed quickly into tensile cracks, and the earliest observed one was near the steep surface and continued developing into the longest one. As new tensile cracks continued developing towards the inner of the slope, the slip surface developed, the lower part of the slope body gradually separated from the main slope body, and landslide occurred under the high hydraulic gradient of pressure.

7 Concluding remarks

The change of water level can cause the increase of the gradient of pore water pressure, which induces the seepage within the slope body. The seepage velocity responds directly to the hydraulic pressure. Based on the simulating experiment on drawdown of water level in the lower reach of a layered slope, the seepage field, the distribution of the pore water pressure, and the field of the gradient of water head within the slope model were computed. The computing results were compared with the results from experimental observation and measurement, and the two results were essentially in agreement. The results showed that the slope would become instable after the fall of the water level in the lower reach, because the high gradient of pore water pressure would develop near the foot of the slope. Thus, as the part of the steep slope surface above water level was exposed more and more, the deformation initiated, the slip surface developed, and the landslide occurred under the action of dynamic seepage pressure and the static water pressure. The mechanism of landslide for such a kind of slopes is then probed and clarified. In practical slope engineering, the reasonable design for drainage system and reinforcement for the foot of the slope are necessary to prevent collapse or landslide induced by drawdown of water level.

Acknowledgements The authors wish to thank all their colleagues in the Institute of Mechanics, CAS, for their valuable discussion on various parts of the work described in the paper. This work was supported by the National Natural Science Foundation of China (Grant No. 10372104), the Special Funds for the Major State Basic Research Project (Grant No. 2002CB412706), the Knowledge Innovation Project of the Chinese Academy of Sciences (Grant No. KJCX2-SW-L1-2), the Special Research Project for Landslide and Bank-collapse in The Three Gorges Reservoir Areas (Grant No. 4—5).

References

1. Trollope, D. H., The Vaiont slope failure[J], Rock Mechanics, 1980, 13(2): 71—88.
2. Cui Zhengquan, Li Ning, Slope Engineering—New Advancement in Theory and Practice[M], Beijing: China Water Power Press (in Chinese), 1999.
3. Cai Yaojun, Cui Zhengquan, Cojean R., Mechanism on deformation and instability of bank slope induced by reservoir[A], in Proceeding of the 6th National Conference of Rock Mechanics and Engineering[C], Beijing: China Science and Technology Press (in Chinese), 2000, 618—622.
4. Ding Enbao, Problems of super-high and steep slopes in development of hydroelectric power on Jinshajiang river[J], Journal of Engineering Geology (in Chinese), 2000, 8(2): 131—135.
5. Cheng Chiyuan, The analysis and treatment on the landslide of the dam of Dayuanhe reservoir[J], Jiangxi Hydraulic Science and Technology (in Chinese), 1992, 18(3): 207—210.
6. Tang Weizeng, The accident analysis that reservoir drainage result in sliding for earthfill dam's upstream face[J], Jiangxi Hydraulic Science and Technology (in Chinese), 1992, 21(4): 197—202.
7. Deng Jianhui, Ma Shuishan, Zhang Baojun et al., Preliminary investigation on the reactivation of Maoping landslide, Geheyan Reservoir, Qingjiang River[J], Chinese Journal of Rock Mechanics and Engineering (in Chinese), 2003, 22(10): 1730—1737.
8. Wang Shangqing, Yi Qinglin, Yan Xueqing, The synthetic analysis on deformation characteristics and influential factors of Maoping landslide, Qingjiang[J], The Chinese Journal of Geological Hazard and Control (in Chinese), 1999, 10(2): 40—44.
9. Zhang Junfeng, Meng Xiangyue, Zhu Erqian, Testing study on landslide of layered slope induced by fluctuation of water level[J], Chinese Journal of Rock Mechanics and Engineering (in Chinese), 2004, 23(16): 2676—2680.
10. Enoki, M., Kokubu, A. A., Ikeda, Y., Infiltration of rainwater and slope failure[A], in Proceedings of the Ninth International Conference and Field Trip on Landslides[C] (eds., James S. Griffiths, Martin R. Stokes, Robbert G. Thomas), Rotterdam: A. A. Balkema, 1999, 27—35.